



## PtSnNa@SUZ-4-catalyzed propane dehydrogenation

Hualan Zhou<sup>a</sup>, Jingjing Gong<sup>a</sup>, Bolian Xu<sup>a</sup>, Lei Yu<sup>a,b</sup>, Yining Fan<sup>a,\*</sup><sup>a</sup> Key Laboratory of Mesoscopic Chemistry of MOE, Jiangsu Provincial Key Laboratory of Nanotechnology, School of Chemistry and Chemical Engineering, Nanjing University, Nanjing, 210093, China, China<sup>b</sup> Jiangsu Key Laboratory of Environmental Material and Environmental Engineering, School of Chemistry and Chemical Engineering, Yangzhou University, Yangzhou, 225002, China, China

## ARTICLE INFO

## Article history:

Received 14 June 2016

Received in revised form 15 August 2016

Accepted 20 August 2016

Available online 22 August 2016

## Keywords:

SUZ-4 zeolite

PtSn

Sodium

Propane dehydrogenation

Propylene

## ABSTRACT

SUZ-4-based Pt-Sn catalysts with different sodium ion contents were prepared through sequential impregnation method. The structural and catalytic properties of the catalysts were studied by using various techniques combined with micro-reactor tests. The experimental results showed that PtSnNa/SUZ-4 catalysts exhibited high durability, high propylene selectivity and high stability with adequate sodium ion content. Sodium ion additives neutralized the strong acid sites and prevented the formation of coke. However, excess sodium ion not only reduced tin species to metallic tin, which reduced the catalyst activity by forming PtSn alloys, but also led to more Pt particles inside the pore of zeolite, which were easily deactivated by coke. It was found that catalysts with the sodium ion content at 0.5–1.5wt% led to the highest propane conversion and propylene selectivity.

© 2016 Elsevier B.V. All rights reserved.

## 1. Introduction

Bimetallic platinum-tin (Pt-Sn)-based catalysts have attracted much attention for their industrial application potential in recent years. [1–3]. They have been widely employed in many reactions, such as light paraffin dehydrogenation [1,4,5], alcohol oxidation [6,7] and the hydrogenation for carbonyl compounds [8,9] et al. Among these applications, dehydrogenation of propane to produce propylene is a significant petrochemical process for the rapidly increasing demand of propylene [10,11]. However, current reaction conditions suffer high temperature and low H<sub>2</sub> partial pressure, which leads to undesirable thermal cracking reactions to coke and light alkanes and results in low product yield and eventually deactivation of the catalyst [11–13]. Therefore, developing an efficient catalyst with high activity, high stability and high propylene selectivity is urgently required. The conventionally employed PtSn/γ-Al<sub>2</sub>O<sub>3</sub> is considered to be one of the most efficient catalysts for propane dehydrogenation, but is deficiency for their poor stability and weak durability after recoveries [10,14,15]. To resolve the problem, additives, including alkali metals (K, Na) and rare earth metals (La, Ce) have been employed to improve the catalysts [14,16–18].

Yet, zeolite has been used as support for Pt-Sn-based catalysts owing to its high surface area, high thermal stability and tunable Si/Al ratio [3]. Among these materials, SUZ-4 is a novel zeolite patented by the British Petroleum Company in 1992. The three dimensional topological structure of this material has straight ten-membered channels intersected by two eight-membered channels at an angle of about 74°, similar to that of ZSM-5 zeolite [19–21]. H-SUZ-4 zeolite possess large amount of Brønsted acid sites stronger than those on H-ZSM-5 zeolite [22]. Therefore, it has presented considerably high catalytic activity in many reactions, such as conversion of *n*-hexane [20], the synthesis of dimethyl ether from methanol [23], and the elimination of nitrogen oxides [22,24]. SUZ-4 zeolite-supported catalysts might be employed in propane dehydrogenation. But up to present, few studies have been reported in the field while the ZSM-5-supported catalysts have attracted much attention. Compared with γ-Al<sub>2</sub>O<sub>3</sub>, ZSM-5 zeolite possesses a special three dimensional topological structure, which can inhibit the production of large hydrocarbon molecules to suppress the coke deposits and enhance the catalyst stability [25]. Recently, Zhou *et al* investigated the effect of promoters of PtSn/ZSM-5 catalyst for propane dehydrogenation and found that introduction of the third or fourth promoter (K, La) could improve the catalyst activity by decreasing the acid sites of the support and strengthening the interaction between Sn and the carrier [26,27]. In this paper, we employed SUZ-4 zeolite-supported PtSn catalysts in propane dehydrogenation with sodium ion as the additive to improve the catalyst. The effects of sodium ion addition were carefully inves-

\* Corresponding author.

E-mail addresses: [ynfan@nju.edu.cn](mailto:ynfan@nju.edu.cn), [yulei@yzu.edu.cn](mailto:yulei@yzu.edu.cn) (Y. Fan).

tigated by testing a series of catalysts with different sodium ion contents in propane dehydrogenation. Herein, we wish to report our findings.

## 2. Experimental

### 2.1. Catalyst preparation

SUZ-4 zeolite was prepared by the hydrothermal crystallization method, as described in literature [28]. The solid phase obtained was filtered, washed with distilled water for several times, dried at 110 °C for 12 h and then calcined at 550 °C for 4 h, followed by NH<sub>4</sub><sup>+</sup>-exchange with 1 M aqueous NH<sub>4</sub>Cl. H-SUZ-4 was obtained by calcining the ammonium form of SUZ-4 at 550 °C for 4 h. The PtSnNa catalysts supported on SUZ-4 zeolite (Pt 0.5wt%, Sn 2.0wt%, Na 0–2.0wt%) were prepared by impregnating H-SUZ-4 into (H<sub>2</sub>PtCl<sub>6</sub> + SnCl<sub>4</sub>) aqueous mixture (H<sub>2</sub>PtCl<sub>6</sub> 5 mg/ml, SnCl<sub>4</sub> 5.85 mg/ml) and aqueous NaCl (0.5 mol/L) respectively in order. The samples were dried at 110 °C for 4 h, calcined in air at 520 °C for 4 h, and then dechlorinated in air containing water vapor at 530 °C for 4 h. The PtSnNa catalyst with different sodium ion content was described as PtSnNa(m)/SUZ-4 (m = 0.5, 1, 1.5 and 2) in the whole paper.

### 2.2. Catalyst characterization

The powder X-ray diffraction (XRD) patterns of all samples were obtained on a Philips X'pert pro diffractometer using Cu K $\alpha$  radiation at 40 kV and 40 mA, from 5° to 50°.

The surface area was calculated by the BET method according to N<sub>2</sub> adsorption isotherms recorded at the temperature of liquid nitrogen using a Micromeritics ASAP2010 analyzer. The samples were degassed at 300 °C and 1 × 10<sup>-3</sup> Torr before analysis, then measured at 196 °C.

H<sub>2</sub> chemisorption on supported catalysts before and after propane dehydrogenation reaction was carried out according to the procedure described in the literature [29]. All catalyst samples were reduced in H<sub>2</sub> flow at 500 °C for 2 h and then out-gassed in an Ar flow at 540 °C for 2 h before H<sub>2</sub> chemisorption measurements.

NH<sub>3</sub>-TPD profiles of the samples were carried out in a flow-type fixed-bed reactor at the ambient pressure. The catalysts were pre-treated at 500 °C for 2 h in argon flow. The NH<sub>3</sub> adsorption temperature was 100 °C, and the temperature was raised at a rate of 10 °C/min. The desorbed NH<sub>3</sub> was detected by gas chromatography equipped with TCD.

The amount of carbon deposited on the catalysts during propane dehydrogenation reaction was measured by using thermogravimetric (TG) analysis (STA 449C-Thermal star 300 TA-MS apparatus). The catalyst samples (ca. 0.02 g) after reaction for 10 h were heated from room temperature to 900 °C in O<sub>2</sub> (25 ml/min) with heating rate of 10 °C/min, and the amount of coke was calculated from TG curves.

Temperature-programmed oxidation (TPO) was measured with the same apparatus as used for H<sub>2</sub> chemisorption experiments. About 0.1 g of sample was placed in a quartz reactor and then heated up to 800 °C in O<sub>2</sub> (3.0 ml/min) and Ar (30 ml/min) mixture with a rate of 10 °C/min.

Temperature-programmed reduction (TPR) was measured with the same apparatus as used for TPO experiments. About 0.1 g of sample was placed in a quartz reactor and then performed in a flow of 5% H<sub>2</sub>/Ar (20 ml/min) with heating rate of 10 °C/min.

The poisoned catalysts (S 0.02wt%) were prepared by impregnating the reduced PtSnNa/SUZ-4 catalyst into the ethanol solution of dibenzo[*b,d*]thiophene and flushed with nitrogen. The samples were dried at 110 °C for 4 h.

**Table 1**

The pore volume, surface area, H<sub>2</sub> uptake and the amount of coke deposits on the different samples<sup>a</sup>.

Entry	Cat.	V <sub>P</sub> <sup>b</sup>	S <sub>BET</sub> <sup>c</sup>	H <sup>d</sup>	C <sup>e</sup>
1	H-SUZ-4	0.195	378	–	–
2	PtSn/SUZ-4	0.181	339	8 (3)	14.5
3	PtSnNa(0.5)/SUZ-4	0.162	322	19 (12)	9
4	PtSnNa(1.0)/SUZ-4	0.160 (0.114)	319 (213)	22 (19)	8
5	PtSnNa(1.5)/SUZ-4	0.153	310	21 (18)	8
6	PtSnNa(2.0)/SUZ-4	0.152	280	15 (8)	6.8

<sup>a</sup> Data in parenthesis are the value for catalysts after reaction for 10 h.

<sup>b</sup> Pore volume (cm<sup>3</sup>/g).

<sup>c</sup> BET surface area (m<sup>2</sup>/g).

<sup>d</sup> H<sub>2</sub> uptake (ml/gPt).

<sup>e</sup> Coke amount (wt%).

All catalysts were reduced in H<sub>2</sub> at 500 °C for 2 h before catalytic evaluation. The propane dehydrogenation reaction was carried out in a quartz tubular micro-reactor under reaction conditions of 0.1 MPa, 590 °C, C<sub>3</sub>H<sub>8</sub>/H<sub>2</sub> = 1/3 (molar ratio) and the weight hourly space velocity (WHSV) of propane was 3.0 h<sup>-1</sup>. The reaction products (C<sub>3</sub>H<sub>6</sub>, CH<sub>4</sub>, C<sub>2</sub>H<sub>6</sub> and C<sub>2</sub>H<sub>4</sub>) were analyzed by an online gas chromatography (Shimadzu GC-14A, Japan) with a thermal conductivity detector and an Al<sub>2</sub>O<sub>3</sub> packed column.

## 3. Results and discussion

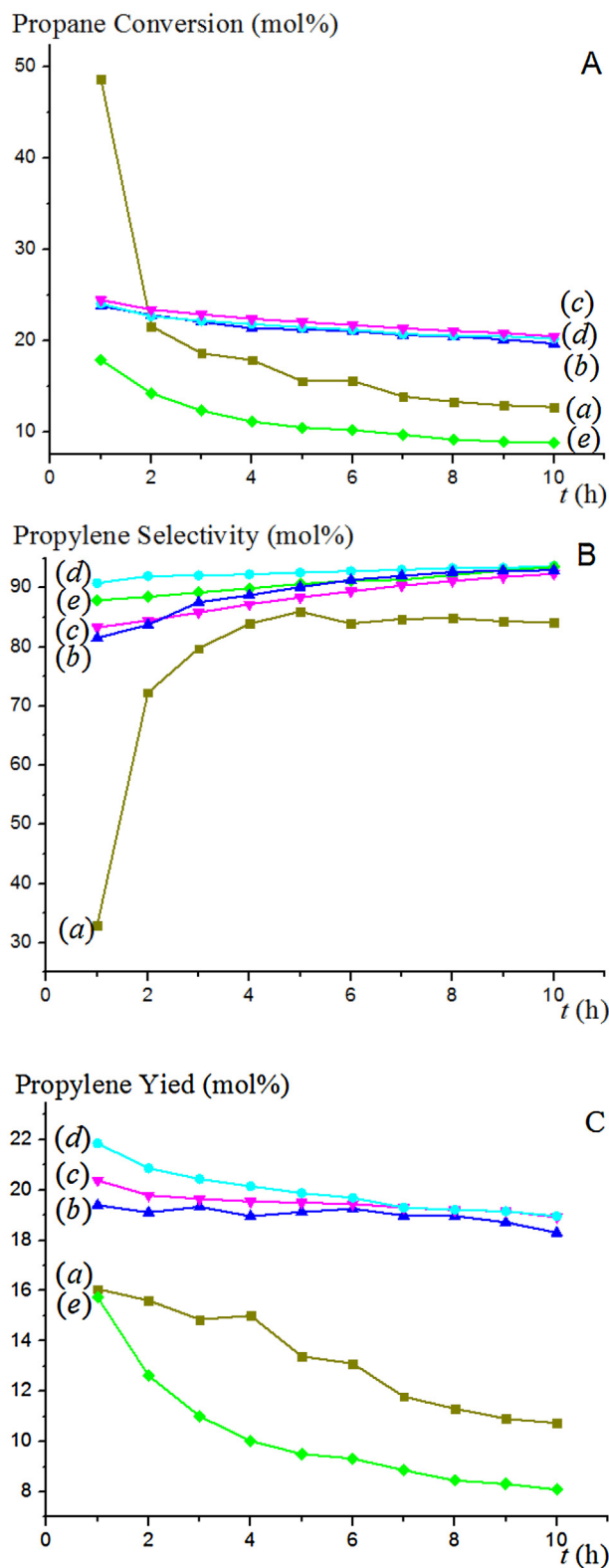
### 3.1. Propane dehydrogenation

A series of catalysts with different sodium ion contents were employed in propane dehydrogenation. As shown in Fig. 1, PtSn/SUZ-4 catalyst exhibited high initial reaction activities but poor propylene selectivity because of side reactions (cracking, isomerization and polymerization). It posed very poor stability, which was manifested by the quickly decreased propane conversion caused by the catalyst deactivation (Fig. 1A, curve *a*; Fig. 1B, curve *a*). The PtSnNa catalysts, exhibited lower initial propane conversion but were more durable. Obviously, sodium ion as additive largely improved the catalyst durability, which led to the stable high propane conversion (Fig. 1A, curves *b–e* vs. *a*) and high propylene yields (Fig. 1C, curves *b–d* vs. *a*), but the reactivity especially the initial reactivity of the catalyst was lowered. Excess sodium ion was harmful on the contrary and it was found that within 1.5wt% content of the sodium ion was favorable (Fig. 1C, curves *b–d* vs. *e*).

### 3.2. Structure and surface properties of the catalysts

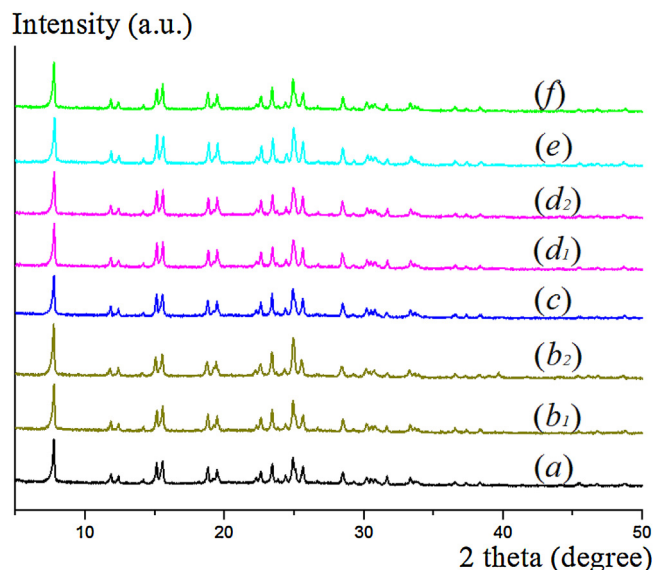
X-ray diffractions (XRD) experiments of the materials were then performed. As shown in Fig. 2, no signals of Pt, Sn or Na were observed after the impregnation, possibly due to their low concentration and/or the high dispersion states of these metal elements (Fig. 2, curves *b*<sub>1</sub>, *c*, *d*<sub>1</sub>, *e* and *f*) [25]. Moreover, compared with the original structure of SUZ-4 zeolite, the XRD patterns of the supported catalysts did not show any characteristic changes (Fig. 2, curves *a* vs. *b–f*). After the propane dehydrogenation reaction for 10 h, the signals of SUZ-4 zeolite were also observed in the catalysts, as shown in Fig. 2, curves *b*<sub>2</sub> and *d*<sub>2</sub>, which indicated the structure of the supports was not destructed during the reaction.

Table 1 affords the characterization data of the different catalysts. It was shown that the pore volume (V<sub>p</sub>) and surface area decreased in supported catalysts and these values further went down after the reaction (Table 1, entries 2–6 vs. 1). The phenomena might be caused by the occupation of the catalyst metal Pt or coke on support pores. And among these supported catalysts, the surface area of PtSnNa(2.0)/SUZ-4 was the smallest one (entry 6). H<sub>2</sub> uptake of the fresh PtSnNa/SUZ-4 catalyst increased with the sodium ion content before 1.0wt%. It is shown that sodium ion additives were



**Fig. 1.** Propane conversion (A); propylene selectivity (B) and propylene yield (C) as a function of reaction time for different catalysts: (a) PtSn/SUZ-4, (b) PtSnNa(0.5)/SUZ-4, (c) PtSnNa(1.0)/SUZ-4, (d) PtSnNa(1.5)/SUZ-4 and (e) PtSnNa(2.0)/SUZ-4. Reaction conditions: 590 °C,  $H_2/C_3H_8 = 1/3$  (molar ratio),  $m$  (cat.) = 0.3 g,  $WHSV = 3.0 h^{-1}$ .

beneficial to improve the dispersion of Pt. Compared with fresh catalyst,  $H_2$  uptake decreased after the reaction because of the coke deposition.  $H_2$  uptake of the fresh PtSn/SUZ-4 catalyst (8 ml/gPt) was in consistent with the catalytic activity in the initial reaction



**Fig. 2.** XRD patterns of different samples. (a) H-SUZ-4, (b<sub>1</sub>) PtSn/SUZ-4, (b<sub>2</sub>) the (b<sub>1</sub>) after 10 h reaction, (c) PtSnNa(0.5)/SUZ-4, (d<sub>1</sub>) PtSnNa(1.0)/SUZ-4, (d<sub>2</sub>) the (d<sub>1</sub>) after 10 h reaction, (e) PtSnNa(1.5)/SUZ-4 and (f) PtSnNa(2.0)/SUZ-4.

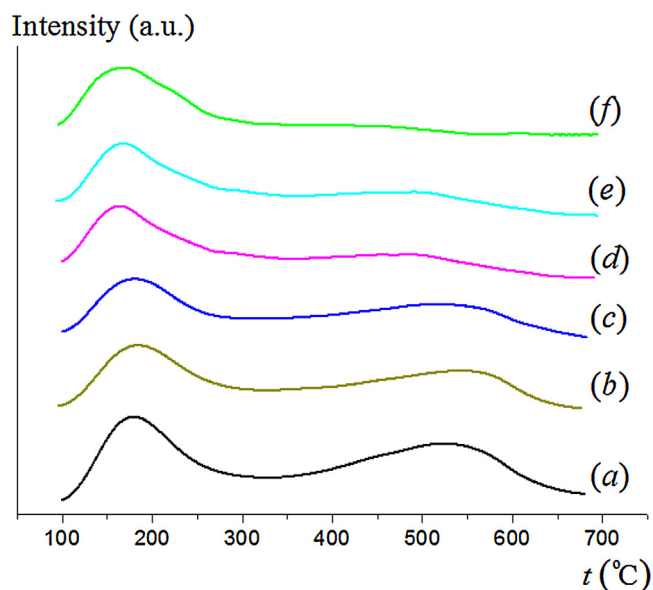


**Fig. 3.**  $NH_3$ -TPD profiles of the samples. (a) H-SUZ-4, (b) PtSn/SUZ-4, (c) PtSnNa(0.5)/SUZ-4, (d) PtSnNa(1.0)/SUZ-4, (e) PtSnNa(1.5)/SUZ-4 and (f) PtSnNa(2.0)/SUZ-4.

stage (Fig. 1A, curve e), but gradually reduced dramatically after coke deposits (3 ml/gPt, Table 1, entry 2).

Generally, sodium ion additives largely affected the acid sites of zeolite and the catalyst performances. The acidity of the different catalysts was examined by temperature-programmed desorption (TPD) of ammonia experiments. The  $NH_3$ -TPD profiles were displayed in Fig. 3 while the detailed data were shown in Table 2. Two ammonia desorption peaks appeared in TPD profiles for H-SUZ-4 and supported catalysts. The first signal at ca. 180–190 °C was attributed to be the weak acid absorption, while the second peak at ca. 420–560 °C indicated the strong acid sites (curve a) [30]. With the sodium ion content increasing, peak temperature and peak area at 180 °C were little changed. But the strong acid site peaks moved to low-temperature direction and were gradually weakened (curves b–f). Particularly, in PtSnNa(2.0)/SUZ-4, strong

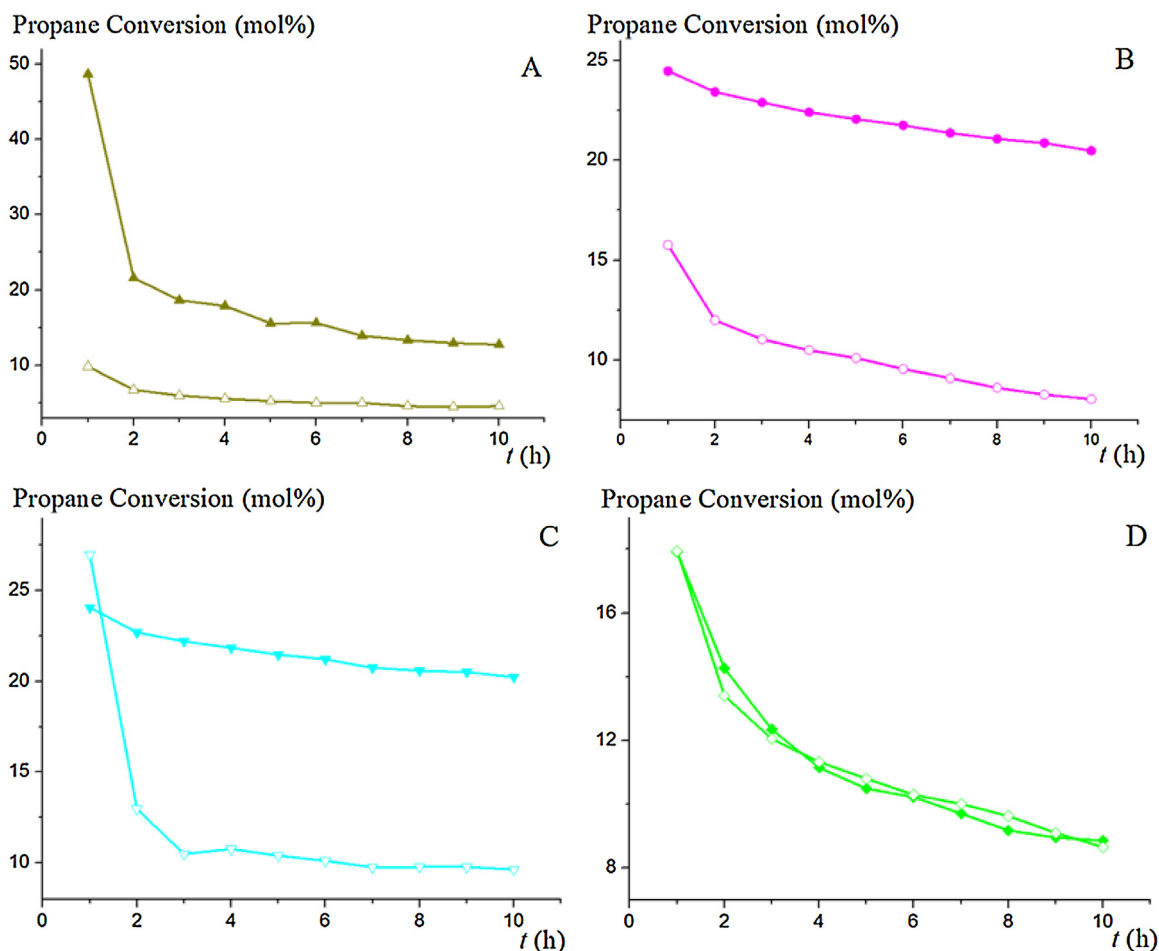


**Fig. 4.** The propane conversion of different catalysts before (filled) and after *pre-treatment* experiment with dibenzo[b,d]thiophene (opened): (A) PtSn/SUZ-4, (B) PtSnNa(1.0)/SUZ-4, (C) PtSnNa(1.5)/SUZ-4 and (D) PtSnNa(2.0)/SUZ-4.

**Table 2**

The acid amount calculated from the corresponding desorption peak area in Fig. 4 for different catalysts.

Entry	Curve <sup>a</sup>	Cat.	Acid Amount		
			Weak	Strong	Total
1	<i>a</i>	H-SUZ-4	389	587	976
2	<i>b</i>	PtSn/SUZ-4	349	360	709
3	<i>c</i>	PtSnNa(0.5)/SUZ-4	350	305	655
4	<i>d</i>	PtSnNa(1.0)/SUZ-4	354	297	651
5	<i>e</i>	PtSnNa(1.5)/SUZ-4	382	270	652
6	<i>f</i>	PtSnNa(2.0)/SUZ-4	513	0	513

<sup>a</sup> Curves in Fig. 3.

acid site peak disappeared (curve *f*). As the peak area of a TPD profile represented the amount of desorbed  $\text{NH}_3$  (calculate from the total desorption peak area), whereas the peak position displayed the strength of acidity, the addition of tin and sodium promoters could neutralize the strong acid sites of zeolites preferentially, and led to the reduced amount and intensity of the strong acid sites. Generally, the surface area and acid sites of zeolite with regular pore structure are mainly provided by its inner surface. Pt metal particles disperse on both the outside and inner surface of zeolite. Pt acid precursor ( $\text{H}_2\text{PtCl}_6$ ) is prevented to enter the SUZ-4 channel because of stronger acid strength of SUZ-4 zeolite [31]. But the addition of sodium ion can neutralize the strong acid sites and promotes the dispersion and combination of the catalyst precursor into the inner surface of SUZ-4, leading to the decrease of the surface area and pore volume of the catalyst.

In dehydrogenation processes, side reactions (cracking, isomerization and polymerization) are mainly catalyzed by strong acid sites. Thus, neutralization of the strong acid sites reduces the undesirable side-reactions and improves propylene selectivity [32]. As shown in Fig. 1B and Table 1, propylene selectivities increased and the coke amount decreased along with the sodium ion content addition, which might be attributed to the reduction of acid sites in the PtSnNa/SUZ-4 catalysts shown in Fig. 3 and Table 2. However, in PtSnNa(2.0)/SUZ-4, although the coke amount decreased to 6.8 (Table 1, entry 6), the conversion of propane declined to 8.7 mol% (Fig. 1A, curve *e*). Thus, it was suggested that the amount of coke deposits affected by the sodium ion addition was a significant reason but not the only one for the variation of catalyst activity.

### 3.3. Pre-treatment experiment with dibenzo[b,d]thiophene

To investigate the detailed structure of the materials, experiments using dibenzo[b,d]thiophene-poisoned catalysts were tested. As shown in Fig. 4, for all of the PtSn/SUZ-4, PtSnNa(1.0)/SUZ-4 and PtSnNa(1.5)/SUZ-4 catalysts, their activities decreased after treating with dibenzo[b,d]thiophene (Figs. 4A, B and C), but the activity of PtSnNa(2.0)/SUZ-4 was nearly unchanged after being treated with dibenzo[b,d]thiophene (Fig. 4D). Because dibenzo[b,d]thiophene had larger molecule diameter (*ca.* 0.8 nm) than the tunnels of SUZ-4 zeolite (*ca.* 0.46–0.52 nm) [29,33], it could only contact with the surface Pt catalyst, while the catalyst Pt particles inside the tunnels remained untouched. Therefore, the proportion of Pt inside the pores of zeolite can be analyzed

**Table 3**

The propane conversion of the catalysts before and after poisoning experiment after reaction for 10 h, and the ratio of propane conversion between the fresh and poisoning catalysts (P/F).

Entry	Catalyst	Propane conversion after 10 h (mol%)		Ratio P/F
		Fresh	Poisoning	
1	PtSn/SUZ-4	12.8	4.59	0.359
2	PtSnNa(1.0)/SUZ-4	20.5	8.05	0.393
3	PtSnNa(1.5)/SUZ-4	20.2	9.63	0.477
4	PtSnNa(2.0)/SUZ-4	8.86	8.66	0.977

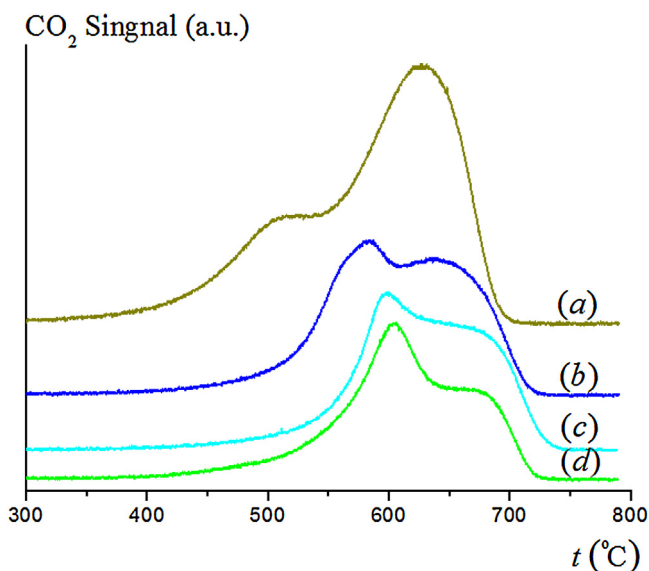


**Fig. 5.** TPO profiles of different samples: (a) PtSn/SUZ-4, (b) PtSnNa(0.5)/SUZ-4, (c) PtSnNa(1.5)/SUZ-4 and (d) PtSnNa(2.0)/SUZ-4.

by the ratio of propane conversion between the reactions with dibenzo[*b,d*]thiophene-poisoned catalysts and fresh ones (P/F). As shown in Table 3, the ratio of P/F increased with the sodium ion addition, indicating the increased Pt dispersion inside the channels. When PtSnNa(2.0)/SUZ-4 was employed, almost all of the Pt particles went into the channel of zeolite, resulting in a sharp drop in surface area, and under these conditions, the carbon deposits could easily block the channels of SUZ-4 and deactivate the catalysts (Table 1, entry 6). The phenomena were caused by the neutralization of the stronger acid sites of SUZ-4 zeolite, which prevented the Pt acid precursor ( $H_2PtCl_6$ ) entering into the SUZ-4 channel.

The differences of Pt distribution inside and outside the channels of the catalysts might lead to the different distribution of carbon deposition. Temperature-programmed-oxidation (TPO) profiles of different catalysts were illustrated in Fig. 5. For PtSn/SUZ-4 catalyst, two successive peaks representing different carbon deposits were observed. The first peak at ca. 520°C should be attributed to carbon deposits that covered the catalyst metal Pt, while the second peak at higher ca. 630°C was for the carbon deposit located on zeolite surface, as in good agreement with the reported literature (curve a) [2]. It is worth noting that the high temperature peaks split with the addition of sodium ion (curves *b–d* vs. *a*). Considering the experimental results of *pre-treatment* experiment with dibenzo[*b,d*]thiophene (Fig. 4), the peaks at low temperature in the PtSnNa(*m*)/SUZ-4 catalysts were probably ascribed to carbon deposits that cover the Pt surface inside the zeolite pores, while the peaks at high temperature could be attributed to the carbon deposit in zeolite channels (curves *b–d*). Hence, sodium ion additives might modify Pt distribution in the catalysts, and thus affected

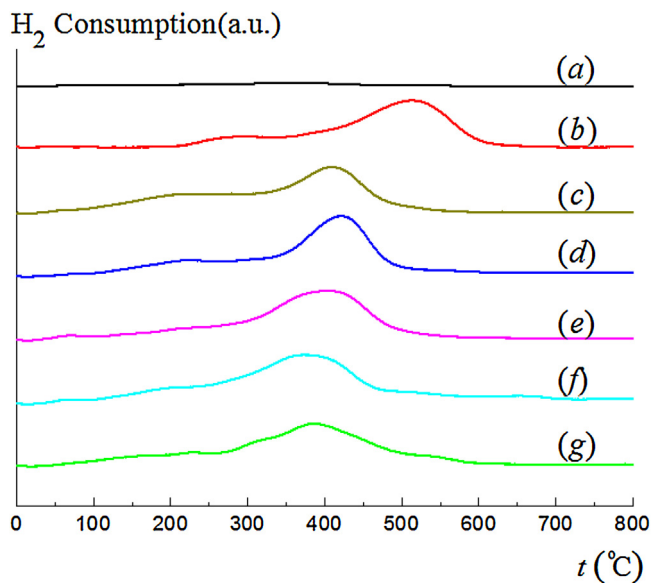


**Fig. 6.**  $H_2$ -TPR profiles of different samples. (a) Pt/SUZ-4, (b) Sn/SUZ-4, (c) PtSn/SUZ-4, (d) PtSnNa(0.5)/SUZ-4, (e) PtSnNa(1.0)/SUZ-4, (f) PtSnNa(1.5)/SUZ-4 and (g) PtSnNa(2.0)/SUZ-4.

the coke distribution on zeolite and greatly affected the catalyst performances in propane dehydrogenation.

#### 3.4. Interaction of catalyst components

Previous studies have indicated that the interaction between Pt-Sn-support was an important factor that affected the state of the Sn component, the state of the Pt dispersion and the dehydrogenation performance of the catalyst [34,35]. For catalysts with high content of metal components but low dispersion, it is difficult to get enough information on the catalyst active phase structure through XRD and XPS methods. In order to further disclose the interaction of each component in the PtSnNa supported catalysts, temperature-programmed-reactions (TPR) with  $H_2$  were then investigated. As shown in Fig. 6, a broad but weak reduction peak was observed at 350°C for Pt/SUZ-4 sample, indicating that most Pt(II) decomposed to Pt(0) after calcination (curve a) [36]. For Sn/SUZ-4, two TPR peaks were observed: the peak at 300°C was attributed to be the reduction of Sn(IV) to Sn(II), while the peak at 520°C clearly indicated the reduction of Sn(IV) or Sn(II) to Sn(0) (curve b) [37]. The addition of Pt made Sn was easier to be reduced, as the signals of PtSn/SUZ-4 moved to low temperature direction (curves *c* vs. *b*). Compared with PtSn/SUZ-4, addition of sodium ions led to the increase of TPR peak area. Moreover, Sn(II) to Sn(0) TPR peak moved to lower temperature, showing that Sn species in the PtSnNa/SUZ-4 was much easier to be reduced to metallic Sn especially for PtSnNa(2.0)/SUZ-4 (curves *d–g* vs. *c*). Then the coverage of surface Pt by metallic Sn species on the Pt-Sn alloys may lead to the decreases of  $H_2$  uptake and reduced catalyst activity for hydrocarbon dehydrogenation [38,39]. Thus, excess sodium ion content in PtSnNa(2.0)/SUZ-4 resulted in poor catalyst performances on the contrary.

#### 4. Conclusions

In conclusion, sodium ion contents neutralized the strong acid sites on SUZ-4 zeolite and enhanced the catalyst durability and propylene selectivity by suppressing the side reactions in propane dehydrogenation processes. Although the reactivity of the catalyst might be lowered at the beginning of the reaction, the propylene selectivity and catalytic stability were largely improved, which

was even more important factors in industrial production. However, over-addition of sodium ion largely deactivated the catalyst because of the decreased surface area and the reduction of Sn(II) to Sn(0), which led to PtSn alloys with Pt and reduced the catalyst activity. Over-addition of sodium ion also led to more Pt clusters inside the pores because of the neutralization of strong acid sites that allowed the entrance of Pt precursor ( $\text{H}_2\text{PtCl}_6$ ) into zeolite channels. Since Pt inside the pores could be easily deactivated by coke deposition, the effect was harmful to catalyst. Therefore, an adequate addition of sodium ion additives is a key factor for the catalyst designing and it was found that addition of 0.5–1.5wt% sodium ion content should be the best protocol in PtSnNa/SUZ-4 catalyst designing.

### Acknowledgment

We thank Jiangsu Planned Projects for Postdoctoral Research Funds (1301080C), NNSFC (21202141), Key Science & Technology Specific Projects of Yangzhou (YZ20122029), the Opening Foundation of the Key Laboratory of Environmental Materials and Engineering of Jiangsu Province (K14010) and Yangzhou Nature Science Foundation (YZ2014040), the Innovation Foundation of Yangzhou University (2015CXJ009) and the High Level Talent Support Project of Yangzhou University for financial support.

### References

- [1] B.K. Vu Song, M.B. Song Ahn, I.Y. Ahn, Y.W. Suh, D.J. Suh, W.I. Kim, H.L. Koh, Y.G. Choi, E.W. Shin, *Appl. Catal. A: Gen.* 400 (2011) 25–33.
- [2] Y.W. Zhang, Y.M. Zhou, K.Z. Yang, A.D. Qiu, Y. Wang, Y. Xu, P.C. Wu, *Catal. Commun.* 7 (2006) 860–866.
- [3] M.S. Kumar, D. Chen, A. Holmen, J.C. Walmesley, *Catal. Today* 142 (2009) 17–23.
- [4] H. Seo, J.K. Lee, U.G. Hon, G. Park, Y.S. Yoo, J. Lee, H. Chang, I.K. Song, *Catal. Commun.* 47 (2014) 22–27.
- [5] A.I. Juez, A.M. Beale, K. Maaßen, T.C. Weng, P. Glatzel, B.M. Weckhuysen, *J. Catal.* 276 (2010) 268–279.
- [6] J. Asgardí, J.C. Calderón, F. Alcaide, A. Querejeta, L. Calvillo, M.J. Lázaro, G. García, E. Pastor, *Appl. Catal. B: Environ.* 168–169 (2015) 33–41.
- [7] N. Erini, R. Loukrakpam, V. Petkov, E.A. Baranova, R.Z. Yang, D. Teschner, Y.H. Huang, S.R. Brankovic, P. Strasser, *ACS Catal.* 4 (2014) 1859–1867.
- [8] A.R. Rautio, P.M. Arvela, A. Aho, K. Eränen, K. Kordasa, *Catal. Today* 241 (2015) 170–178.
- [9] K. Zhang, H.T. Zhang, H.F. Ma, W.Y. Ying, D.Y. Fang, *Catal. Lett.* 144 (2014) 691–701.
- [10] X. Liu, W.Z. Lang, L.L. Long, C.L. Hu, L.F. Chu, Y.J. Guo, *J. Chem. Eng.* 247 (2014) 183–192.
- [11] Z. Nawaz, X.P. Tang, Q. Zhang, D.Z. Wang, W. Fei, *Catal. Commun.* 10 (2009) 1925–1930.
- [12] S.M. Stagg, C.A. Querini, W.E. Alvarez, D.E. Resasco, *J. Catal.* 168 (1997) 75–94.
- [13] Z.P. Han, S.R. Li, F. Jiang, T. Wang, X.B. Ma, J.L. Gong, *Nanoscale* 6 (2014) 10000–10008.
- [14] G.D. Angel, A. Bonilla, Y. Peña, J. Navarrete, J.L.G. Fierro, D.R. Acosta, *J. Catal.* 219 (2003) 63–73.
- [15] Y.W. Zhang, Y.M. Zhou, J.J. Shi, S.J. Zhou, X.L. Sheng, Z.W. Zhang, S.M. Xiang, *J. Mol. Catal. A: Chem.* 381 (2014) 138–147.
- [16] C.L. Yu, Q.J. Ge, H.Y. Xu, W.Z. Li, *Appl. Catal. A: Gen.* 315 (2006) 58–67.
- [17] Y.Z. Duan, Y.M. Zhou, Y.W. Zhang, X.L. Sheng, M.W. Xue, *Catal. Lett.* 141 (2011) 120–127.
- [18] S.B. Zhang, Y.M. Zhou, Y.W. Zhang, L. Huang, *Catal. Lett.* 135 (2010) 76–82.
- [19] S.A. Barri, US patent 5118483 (1992).
- [20] D.B. Lukyanov, V.L. Zholobenko, J. Dwyer, S.A.I. Barri, W.J. Smith, *J. Phys. Chem. B.* 103 (1999) 197–202.
- [21] A.C. Gujar, A.A. Moye, P.A. Coghill, D.C. Teeters, K.P. Roberts, G.L. Price, *Micropor. Mesopor. Mater.* 78 (2005) 131–137.
- [22] S. Gao, X.P. Wang, M.R. Li, X.Z. Wang, J. Li, J.P. Feng, *Micropor. Mesopor. Mater.* 183 (2014) 185–191.
- [23] S. Jiang, Y.K. Hwang, S.H. Jhung, J.S. Chang, J.S. Hwang, T.X. Cai, S.E. Park, *Chem. Lett.* 33 (2004) 1048–1049.
- [24] A. Subbiah, B.K. Cho, R.J. Blint, A. Gujar, G.L. Price, J.E. Yie, *Appl. Catal. B* 42 (2003) 155–178.
- [25] Y.W. Zhang, Y.M. Zhou, K.Z. Yang, Y.A. Li, Y. Wang, Y. Xu, P.C. Wu, *Micropor. Mesopor. Mater.* 96 (2006) 245–254.
- [26] S.B. Zhang, Y.M. Zhou, Y.W. Zhang, *Catal. Lett.* 135 (2010) 76–82.
- [27] Y.W. Zhang, Y.M. Zhou, J.J. Shi, S.J. Zhou, Z.W. Zhang, S.C. Zhang, M.P. Guo, *Fuel Process. Technol.* 111 (2013) 94–104.
- [28] H.L. Zhou, Y.J. Wu, W. Zhang, J. Wang, *Mater. Chem. Phys.* 134 (2012) 651–656.
- [29] Z.S. Xu, T. Zhang, Y.N. Fan, L.W. Lin, *Stud. Surf. Sci. Catal.* 112 (1997) 425–432.
- [30] L.J. Lobree, I.C. Hwang, J.A. Reimer, A.T. Bell, *J. Catal.* 186 (1999) 242–253.
- [31] K. Doris, *J. Chem. Educ.* 55 (1978) 459–464.
- [32] C.L. Yu, H.Y. Xu, Q.J. Ge, W.Z. Li, *J. Mol. Catal. A* 266 (2007) 80–87.
- [33] R. Contreras, R. Cuevas-García, J. Ramírez, L. Ruiz-Azuara, A. Gutiérrez-Alejandre, I. Puente-Lee, P. Castillo-Villalón, C. Salcedo-Luna, *Catal. Today* 130 (2008) 320–326.
- [34] J. Salmones, J.A. Wang, J.A. Galicia, G.A. Rios, *J. Mol. Catal. A* 184 (2002) 203–213.
- [35] A. Vázquez-Zavala, A. Ostoa-Montes, D. Acosta, A. Gómez-Cortés, *Appl. Surf. Sci.* 136 (1998) 62–72.
- [36] O.A. Bariás, A. Holmen, E.A. Blekken, *J. Catal.* 158 (1996) 1–12.
- [37] R. Burch, *J. Catal.* 71 (1981) 348–359.
- [38] W.S. Yang, R.A. Wu, L.W. Lin, *Fuel Chem. Technol.* 19 (1991) 200–207.
- [39] W.S. Yang, R.A. Wu, L.W. Lin, *Fuel Chem. Technol.* 19 (1991) 312–319.